TITLE   DYNAMIC BUCKLING OF CONTAINMENTS: THE INFLUENCE OF DAMPING

AUTHOR(S)   Charles Farrar, MEE-13
Thomas Duffey, MEE-13 (Consultant)
Peggy Goldman, MEE-13
Joel Bennett, MEE-13

RECEIVED
FEB 1 1 1993
OSTI

MASTER

Los Alamos   Los Alamos National Laboratory
Los Alamos, New Mexico 87545

DYNAMIC BUCKLING OF CONTAINMENTS:
THE INFLUENCE OF DAMPING

C. R. Farrar, T. A. Duffey, P. A. Goldman, and J. G. Bennett

Los Alamos National Laboratory
Los Alamos, NM 87545 USA

ABSTRACT
The seismic buckling capacities of representative thin, unstiffened elastic containment shells are investigated to evaluate the sensitivity of buckling to the damping level. The finite element method with transient time integration is utilized with both actual earthquake acceleration-time signals and artificial time histories generated from regulatory spectra. The dynamic response and subsequent buckling of the selected containment shells are found to be highly dependent on both damping level and the degree to which the input signal excites the fundamental shear-bending mode of the shell. Transient stresses and buckling levels for the two containment shells induced by the seismic inputs were reduced in the range of 12% to 111% by increasing the damping level from 1% to 4% of critical.

1. INTRODUCTION
Metal containment structures for nuclear reactors are typically thin-walled structures and may be sensitive to buckling because of the combination of conventional dead and live loads as well as seismic excitation. The purpose of this paper is to investigate the influence of damping on the dynamic buckling of thin elastic shells.

Damping values are typically specified in terms of equivalent viscous damping and have been shown to be stress-level dependent. Determination of the role of damping on the response of thin-walled containments is particularly important because of the very low stresses (and associated damping levels) at which these containments buckle. A single viscous modal damping is used for seismic applications, and this value is considered valid for all modes of the structure.

The damping values for welded steel structures given in Table 1 of Regulatory Guide 1.61 [1], are 2% or 4%, with the lower value corresponding to an Operating-Basis Earthquake (OBE), assumed to produce stress levels approximately two-thirds of yield, and the higher value corresponding to a Safe-Shutdown Earthquake (SSE), assumed to produce stress levels approximately 90% of yield [2]. These damping values, as stated in [1], should be used as modal damping values for all modes considered in time-history dynamic analysis. However, [1] also states that if the maximum combined stresses are significantly lower than the yield stress for the SSE, or half the yield stress for the OBE (both of which are the case for the containments analyzed herein), then damping values lower than those specified in [1] should be used to avoid underestimating the amplitudes of vibrations or the amplitude of dynamic stresses.

Newmark and Hall [3] recommend a damping value in the range 0.5% to 1.0% for steel structures at a stress level below one-fourth of the yield stress. More recently [4] they have

recommended a damping value for use at the working stress level (no more than half the yield stress) of 2% to 3%; the 2% value represents a near lower bound and is considered to be "highly conservative."

In 1982 Stevenson and Thomas compared damping values that are used by the U.S., Canada, and Japan [5]. The U.S. nuclear industry uses values between 2% and 4% for welded steel structures. Canada uses 3% and Japan uses 1%.

Recommended or regulatory damping values for metal structures vary over a significant range, and it is important to determine the influence of damping on the buckling of representative containment shells, particularly in view of the low stress (and, therefore, damping) levels at which these containment shells buckle. The investigation is based on design buckling criteria set forth in ASME Code Case N-284.

2. BUCKLING OF CONTAINMENTS: ASME CODE CASE N-284

In 1980, based primarily on work by Miller [6] that summarizes the previous experimental buckling results of others, the ASME adopted Code Case N-284[7]. N-284 presents detailed procedures for the buckling analysis and for the design of metal containment shells. It is based on the assumption that the internal stress field that controls the buckling of the shell consists of the longitudinal membrane (axial), circumferential membrane (hoop), and in-plane shear stresses.

For the case of dynamic loading of a cylindrical shell, the stress results from a dynamic shell analysis (for each time step) are screened for the maximum value of the axial compression, hoop compression, and in-plane shear stress at each area of interest in the shell. The maximum value of each is taken together with the other two concurrent stress components to form a set of quasi-static buckling stress components. For each area of interest on the shell, these three sets of quasi-static buckling stress components corresponding to the three maximum values are used to investigate the buckling capacity of the shell. Interaction curves that provide a means for assessing the buckling capacity of a containment when subjected to a multidimensional state of stress, and formulas for allowable values of stress components that, when acting individually, will cause buckling (intercept values), are presented in N-284.

Tests have shown that geometric imperfections can greatly reduce the buckling capacity of a cylindrical shell. To account for inevitable initial imperfections that will exist in an actual containment structure, "Capacity Reduction" factors are used in N-284 to reduce allowable buckling stress values. The allowable values are effectively reduced further by an appropriate factor of safety, as specified by N-284.

Design interaction surfaces are presented in N-284 to determine whether or not elastic buckling of the containment has occurred. The surfaces are of the general form

$$f\left(\sigma_\phi, \sigma_\theta, \sigma_{\phi\theta}\right) = 1, \tag{1}$$

where σ_ϕ is axial stress, σ_θ is hoop stress, and $\sigma_{\phi\theta}$ is shear stress. Thus, no buckling occurs for $f \leq 1$, whereas the design buckling limit is exceeded for $f > 1$. Here $\sigma_\phi, \sigma_\theta, \sigma_{\phi\theta}$, is the state of stress at a particular point or region on the containment shell at a particular instant in the transient response.

3. NUMERICAL ANALYSIS OF CONTAINMENT SHELLS

Two representative free-standing, unstiffened steel containment shells were selected for analysis. Containment 1 represents a proposed next-generation containment whose geometry is driven by the need for a passive cooling mechanism. Containment 2 is a generic design indicative of

existing unstiffened, free-standing commercial nuclear reactor containments. The geometries of the two selected containments are compared to existing commercial containments in Fig. 1.

3.1 Selection of Analysis Method

A conventional modal analysis was performed with a commercial finite element code [8] to determine the frequencies of the various response modes of the containment shells. Details of the model are given in Subsection 3.3. Results are shown in Fig. 2 for some of the lower shell modes of Containment 1. The fundamental shear-bending mode ($n = 1$, $m = 1$) is seen to occur at approximately 7.1 Hz. Even within a frequency band of 1 Hz about the fundamental shear-bending mode, a large number of shell modes are present. This excessive number of low-frequency shell modes makes solution of the problem by the commonly used modal response spectrum approach impractical. Rather, transient-time integration was chosen, using measured and artificial earthquake acceleration-time histories as input to the base of the structure.

3.2 Specification of Seismic Input

Actual recorded earthquake signals were used in the time history analysis along with artificial histories constructed from regulatory spectra. Various combinations of seismic excitation were applied to the base of the finite element model in the two horizontal directions (global X and Y) and in the vertical direction (global Z). Seismic acceleration-time histories used in this study are the strong motion portions (6-s duration) of the 1940 El Centro N-S component, the 1949 Olympia N86E component, and 1935 Helena west component, scaled to a peak acceleration of 0.3 g's. The strong motion portions of these signals were aligned in time so they would simulate an actual seismic event. In addition, artificial acceleration-time histories were generated from the design spectra given in US NRC Regulatory Guide 1.60.

A correlation analysis was performed between the El Centro and Helena, El Centro and Olympia, and Helena and Olympia acceleration-time histories. It was found that the three signals were uncorrelated (the correlation coefficients all were less than 0.3). Therefore, use of these three different earthquakes assured that the three input components were randomly phased.

3.3 Finite Element Shell Model

An axisymmetric half model of the containment shell as shown in Fig. 3 was generated using a standard 8-node quadratic shell element. Runs were first made to determine the appropriate equilibrium tolerances that were necessary to obtain convergence. The model of Containment 1 was then excited in the Y and Z directions using the Olympia and Helena earthquake acceleration histories, respectively. All vertical (Z) components of acceleration were scaled by a factor of 0.67. A second axisymmetric model was then run, with the El Centro acceleration-time history applied in the Y direction. Results of the time integration of the second run were then rotated 90 degrees (which simulated X-direction excitation) and superposed with the earlier results of the Olympia-Helena run. This superposition of stress components results in the 3-dimensional response of the containment shell from transient base excitation in the three orthogonal directions. Superposition of stress components by this method is valid when the response is small-deflection, elastic behavior.

3.4 Finite Element Results

Results of combined stresses for Containment 1 are shown on the longitudinal compressive shear stress interaction curve in Fig. 4 for 1% damping. The interaction curve is shown in Fig. 4, along with all combined stress points calculated for each time step at integration points near the base. Fig. 4 clearly shows that, for 1% damping, a substantial number of combined stress points lie outside the design interaction curve, implying that the N-284 buckling criteria has been exceeded

for the 0.3 nominal input. Results in Fig. 4 include static loads as well. Using a scaling procedure developed in [9], incipient buckling occurs in this example at 0.17 g.

Results for 4% damping shown in Fig. 5 indicate that the ASME buckling criteria are not exceeded, and that acceleration levels would have to be scaled to a peak value of 0.31 g's to cause incipient buckling. However, for the low stress levels at which buckling occurs for the containment, 4% damping appears inappropriate. Figs. 4-5 again show that buckling of the containment is very sensitive to the damping value chosen.

The hoop component of stress was neglected in Figs. 4-5 to facilitate visualization. If this third component of stress is considered, a 3-dimensional interaction surface results. For example, results for 1% damping, including hoop stresses, are shown in Fig. 6. The points that have been shown are outside the surface and indicate that the N-284 buckling criteria has been exceeded. When the hoop stress component is added, the incipient buckling acceleration level is reduced from 0.17 g's to 0.10 g's, a 59% reduction.

The above superposition procedure was repeated for both Containments 1 and 2 for various other combinations of the El Centro, Olympia, and Helena signals, and for additional acceleration signals including one constructed from regulatory design spectra. Details of the input combinations are presented elsewhere [9].

For a given earthquake combination, the acceleration level required to produce incipient buckling is found to increase with increased damping, as expected. However, the percentage increase in going from 1 to 4% damping varies significantly. The acceleration values for incipient buckling are plotted in Figs. 7-8 as a function of damping level for radius-to-thickness ratios of 645 and 450, respectively. As can be seen, the increase in buckling with damping level is, in all cases, nearly linear, although slopes of the curves -- the sensitivity of damping on buckling -- are different for the various seismic input combinations. These differences are directly attributable to differences in amplification of the fundamental shear-bending mode of the shell.

4. SUMMARY OF RESULTS

A set of finite element numerical analyses of two representative thin-walled steel containment shells are performed using a series of different earthquake signals in various combinations as input. It is found that the acceleration level to produce incipient buckling increases with increased damping. The percentage increase in going from 1% to 4% damping varies significantly and depends on dynamic amplification of the bending-shearing mode of the containment shell. For the various load cases considered, the percentage increase varied between 12% and 111%.

It is clear that buckling of thin containment shells can depend strongly on damping level selected; and that this damping level is a somewhat uncertain value, depending on the stress level. Further effort is needed to assess proper damping levels for dynamic shell buckling.

REFERENCES

1. U. S. AEC Regulatory Guide 1.61, "Damping Values for Seismic Design of Nuclear Power Plants. 1973. Washington, D. C.: U. S. Atomic Energy Commssion.

2. Amin, M., Agrawal, P. K., and Ahl, T. J. 1989. "An Analytical Study of Seismic Threat to Containment Integrity." Washington, D. C.: U. S. Nuclear Regulatory Commission Report NUREG/CR-5098.

3. Newmark, N. M., and Hall, W. J. 1969. "Seismic Design Criteria for Nuclear Reactor Facilities." Proceedings of the Fourth World Conference on Earthquake Engineering, Vol. II, Santiago, Chile.

4. Newmark, N. M., and Hall, W. J. 1978. "Development of Criteria for Seismic Review of Selected Nuclear Power Plants." Washington, D. C.: U. S. Nuclear Regulatory Commission Report, NUREG/CR-0098.

5. Stevenson, J. D., and Thomas, F. A. 1982. "Selected Review of Regulatory Standards and Licensing Issues for Nuclear Power Plants." Washington, D. C.: U. S. Nuclear Regulatory Commission Report, NUREG/CR-3020.

6. Miller, C. D. 1979. "Metal Containment Shell Buckling Design Methods." Plainfield, Illinois: Chicago Bridge and Iron Company.

7. ASME Boiler and Pressure Vessel Code, Section III, Division 1, Case N-284. 1980. "Metal Containment Shell Buckling Design Methods."

8. ABAQUS USER'S MANUAL, Version 4.8. 1989. Hibbitt, Karlsson and Sorensen, Inc.

9. Farrar, C. R., Duffey, T. A., Goldman, P. A., and Bennett, J. G. 1992. "Seismic Buckling Capacity of Unstiffened, Free-Standing Steel Containments." Los Alamos, NM: Los Alamos National Laboratory, LA-12359-MS.
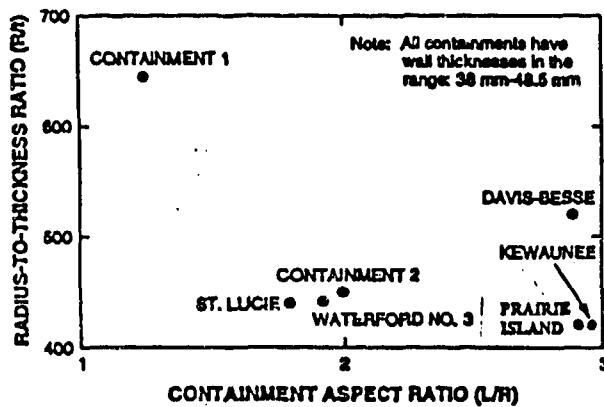
Fig. 1 Comparison of geometries of analyzed containments with existing commerical nuclear reactor containments.
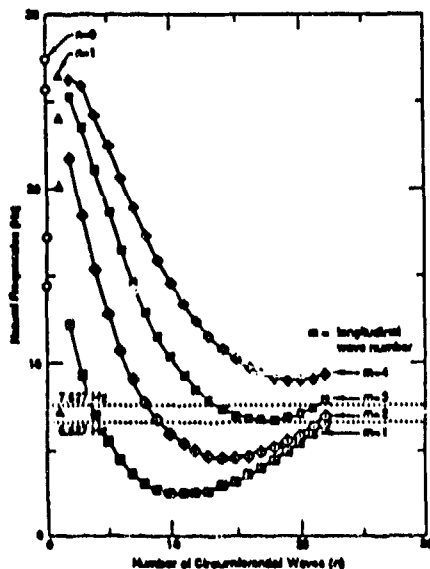

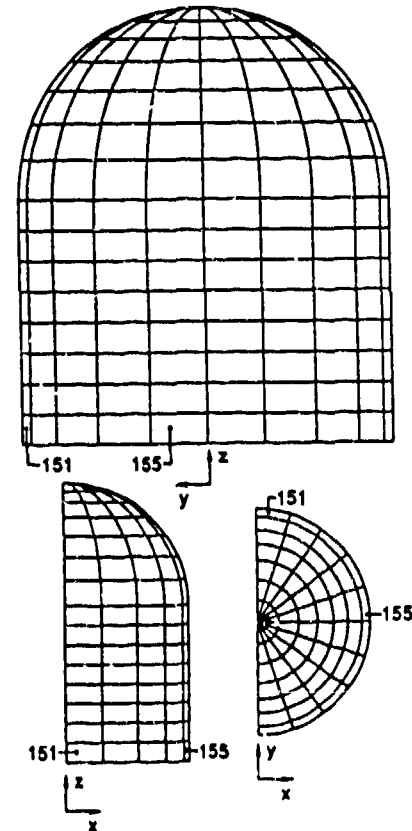Fig. 2 Natural frequencies of the containment structure.

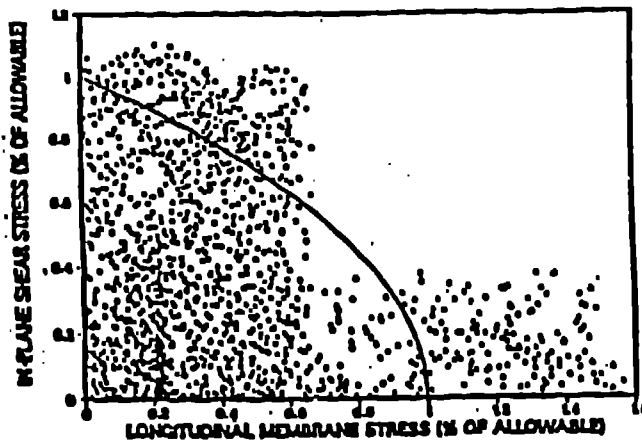Fig. 3 Finite element model of the containment.

Fig. 4   Two-dimensional interaction curve,
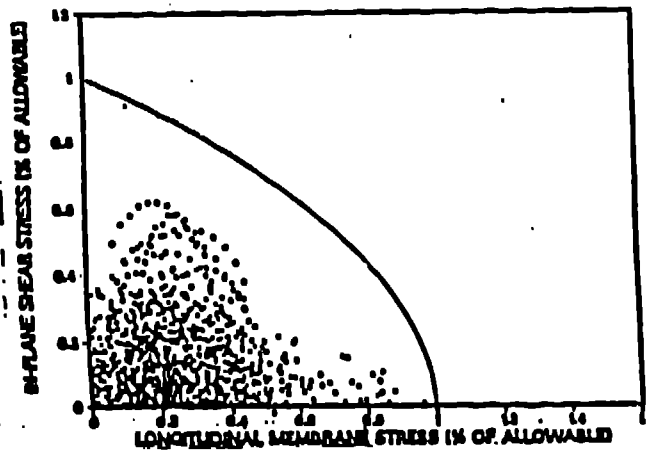   1% damping.

Fig. 7   Influence of damping on the peak
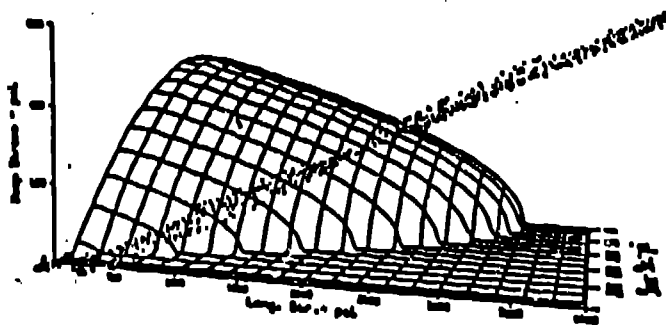   acceleration level that will produce
         a case of incipient buckling in the
         R/t = 645 containment.

Fig. 5   Two-dimensional interaction curve,
         4% damping.

Fig. 8   The influence of damping on the peak
         acceleration level that will produce
         a case of incipient buckling in the
         R/t = 450 containment.

Fig. 6   Three-dimensional interaction curve, 1% damping.
         Only points outside the surface, which indicate
         that the buckling interaction equation has been
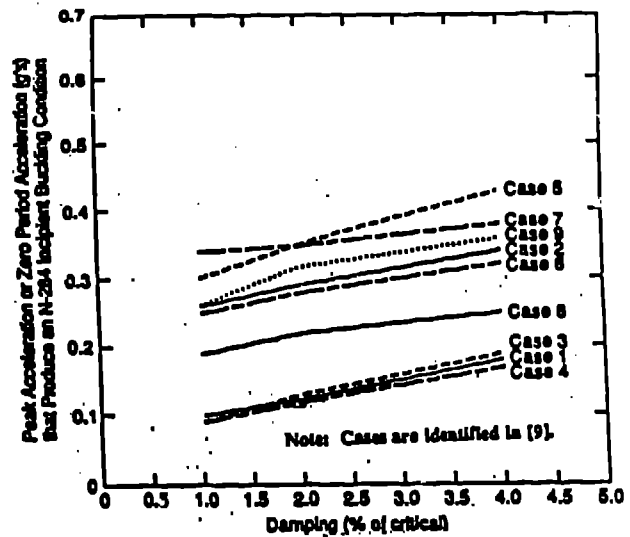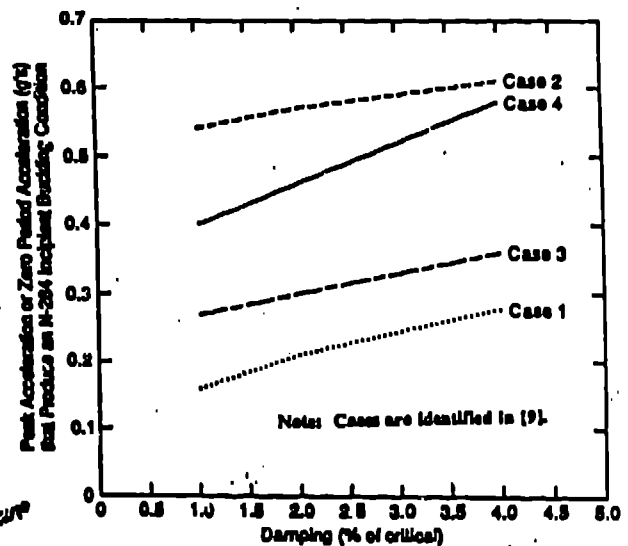   exceeded, are shown.